Numerical Insight into Sound Sources of a Rod-Airfoil Flow Configuration Using Direct Noise Calculation

J. Berland*, P. Lafon†
Laboratoire de Mécanique des Structures Industrielles Durables (LaMSID)
UMR CNRS EDF 2832, Clamart, France

F. Crouzet‡, F. Daude§
Électricité de France R&D
Department of Applied Mechanics and Acoustics, Clamart, France

C. Bailly¶
Laboratoire de Mécanique des Fluides et Acoustique and Institut Universitaire de France
École Centrale de Lyon & UMR CNRS 5509, Ecully, France

The sound radiated by an airfoil in the wake of a rod is predicted by means of compressible large-eddy (LES) simulation. The LES strategy is based on high-order spectral-like numerical methods to allow the direct noise calculation of the sound sources. Owing to the complexity of the geometry, an overset grid approach is implemented in order to tackle with turbulent flows around multiple solid bodies. The aerodynamic data as well as the acoustic far-field are thoroughly compared to the experimental data of Jacob *et al.* [J. Theoret. Comput. Fluid Dyn., 19(3), 2005] in order to demonstrate the accuracy of the present simulation.

I. Introduction

The present work is concerned with the numerical study of the sound generated by an airfoil placed in the wake of a rod. Rod-airfoil configurations are indeed believed to be a benchmark well-suited for numerical modeling of sound generation processes in turbomachines.[17] At appropriate operating conditions, vortex shedding in the wake of the rod can exhibit significant three dimensional effects, and a spectral broadening of the turbulent motions around the shedding frequency commonly occurs.[25] The impingement of these vortical structures on the leading edge of the airfoil generates sound sources, which are similar to the discrete frequency tones and broadband noise observed in turbomachines: rotor blades indeed undergo unsteady pressure fluctuations and one may observe discrete frequency radiation consisting of pure tones at harmonics of the blade passing frequency.[15] In addition, broadband noise is produced by the interaction of the solid surfaces with the turbulent wakes.

The flow physics of the rod-airfoil case has been studied by means of experimental studies. Jacob *et al.*[17] for instance provided an extensive database of the features of the interaction between a cylinder wake and an airfoil. Mean flow quantities, velocity spectra of the turbulent motions as well as pressure spectra in the far-field are available. In a similar manner, Takagi *et al.*[21] investigated the influence of the cylinder

*Ph.D., julien.berland@gmail.com
†Research Engineer, AIAA Senior Member
‡Research Engineer
§Research Engineer
¶Professor, AIAA Senior Member

transverse location (perpendicular to the freestream flow direction) on the turbulent development of the flow around the airfoil and showed that it may have an impact on the radiated acoustic field.

Further knowledge on the details of the rod-airfoil configuration can be gained thanks to numerical simulations. Past developments in the Computational AeroAcoustic (CAA) field have indeed made possible the calculation of the noise radiated by turbulent flows.[24] CAA techniques can be sorted out following two main categories: hybrid and direct approaches. For hybrid calculation, the aerodynamic and the acoustic fields are computed during two separate stages. Turbulence dynamics is first calculated and the radiated sound is then deduced from these data using for instance an acoustic analogy formulation.[18] During the computation of the turbulent flow, noise generation phenomena are not taken into account and classical numerical techniques inherited from computational fluid dynamics can be used. Several attempts have already been made to predict sound spectra radiated by the flow around a rod-airfoil. Casalino *et al.*[8] applied the Ffowcs Williams-Hawkings (FW-H) formulation[13] to flow data provided by an unsteady RANS (Reynolds-Average Navier-Stokes) simulation. In a similar manner, Boudet *et al.*[7] coupled a LES calculation with a FW-H acoustic analogy. More recently, Greschner *et al.*[14] evaluated far-field pressure spectra thanks to a DES/FW-H (Detached Eddy Simulation) aeroacoustic approach. Though these former studies presented results in agreement with the experiments, hybrid methods unfortunately uncouple the aerodynamic and acoustic fields so that the details of the flow physics are more difficult to determine. Both aerodynamic and acoustic fluctuations are computed within a same run for direct approaches. The method, here referred to as direct noise calculation (DNC), does not require any modeling of the sound sources and hence provides reliable results. Even though it has been successfully applied to various flow configurations,[2,5,12] performing a DNC is still a challenging task. High-order numerical techniques on structured grids are commonly used for CAA in order to accurately capture the large disparities of length scales and amplitudes of the aerodynamic and acoustic fluctuations.[22] In the case of flows around multiple bodies, high-order discretization tools are especially tedious to implement. For complex geometries, these difficulties can be circumvented using an overset grid approach.[11] The computational domain is divided into a set of overlapping structured grids. These body-fitted curvilinear meshes greatly ease the enforcement of boundary conditions and allow to simulate flow around various solid bodies. Flow data exchange between the grids can be carried out by means of high-order Lagrangian interpolation.[20] As concern turbulence modeling, the study of flows with Reynolds number of practical interest requires to perform compressible large eddy simulation (LES). In LES, only the larger scales are resolved and a subgrid scale model takes into account the effects of unresolved small wavelengths. It is then possible to deal with realistic turbulence configurations while keeping computational cost at a reasonable level. In the present work, to take account of the dissipation provided by the unresolved scales, a LES based on relaxation filtering (LES-RF) is performed.[6] The idea is to minimize the dissipation at the larger scales while diffusing at small scales the drain of energy due to the turbulence energy cascade. Explicit spectral-like filtering is therefore applied to the conservative flow variables. The method has been successfully used in multiple applications.[2,4]

The present study aims at demonstrating the feasibility of the DNC, based on compressible LES, of the rod-airfoil flow configuration using high-order numerical methods on a set of overlapping structured curvilinear grids. The experimental flow setup of Jacob *et al.*[17] is therefore simulated by *Code_Safari*[12] (Simulation of Aeroacoustics in Flows And with Resonance and Interaction) : a symmetric NACA0012 airfoil is located one chord downstream of a rod, whose wake contains both tonal and broadband fluctuations. The freestream Mach number M_∞ is 0.2.

The outline of this paper is the following. The numerical procedure and the simulation parameters are detailed in section II. The turbulent flow development and the acoustic field of the LES are then investigated in section III. Concluding remarks are drawn in section IV.

II. Simulation setup

II.A. Flow configuration

To allow detailed comparisons to experimental data, the flow configuration for this calculation is taken to be the same of the one used by Jacob *et al.*[17] for their measurements. A sketch of the rod-airfoil setup and of the coordinate system is provided in figure 1. A NACA0012 airfoil is placed in a uniform flow with freestream velocity $U_\infty = 72$ m.s^{-1}, corresponding to a Mach number M_∞ equal to 0.2. A circular rod is located one chord-length upstream the airfoil. The chord length is given by $c_h = 0.1$ m and the rod diameter d is such as $d = c_h/10$. The Reynolds numbers based on the chord length and the rod diameter are respectively given

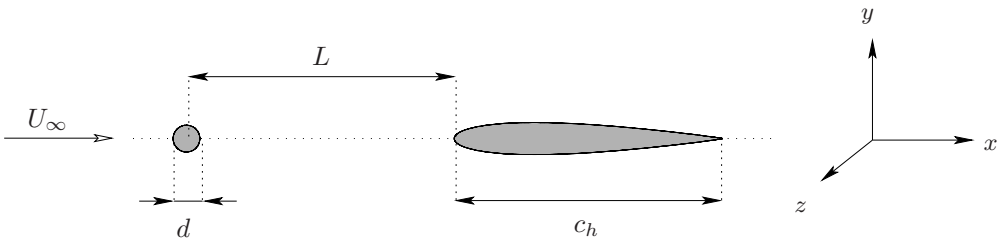

Figure 1. Sketch of the rod-airfoil configuration and of the coordinate system. The diameter of the rod is given by d while c_h is the chord length. The distance between the center of the rod and the leading edge of the airfoil is $L = c_h$. The freestream velocity is U_∞.

Table 1. Detailed characteristics for each mesh of the composite grid.

grid #	type	number of nodes	typical mesh size (m)
1	rod	$500 \times 91 \times 45$	5×10^{-4}
2	airfoil	$400 \times 121 \times 45$	10^{-4}
3	aerodynamic	$1224 \times 189 \times 29$	5×10^{-4}
4	sponge zone	$238 \times 95 \times 29$	10^{-3}
5	intermediate	$1130 \times 189 \times 29$	10^{-3}
6	intermediate	$612 \times 142 \times 15$	2×10^{-3}
7	intermediate	$330 \times 118 \times 8$	4×10^{-3}
8	acoustic	$165 \times 471 \times 4$	10^{-2}

by $\mathrm{Re}_{c_h} = 5 \times 10^5$ and $\mathrm{Re}_d = 5 \times 10^4$.

II.B. Numerical methods and subgrid-scale modeling strategy

Owing to the complexity of the geometry encountered in the present study, an overset (also called Chimera) grid approach has been implemented.[11] The design of overset grids is nonetheless a tedious task since the features of the overlap regions as well as the details of the interpolation procedure have to be established. Numerous grid assembly techniques and softwares are hopefully available[19] and this work makes use of the library *Overture* designed by the Center for Applied Scientific Computing of the Lawrence Livermore National Laboratory.[9]

The three-dimensional unsteady compressible filtered Navier-Stokes equations are solved with the massively-parallel solver *Code_Safari*[12] on the composite grid provided by the library *Overture*.[9] For the purpose of aeroacoustic calculations, the need for highly accurate numerical methods has been recognized since the early stages of this computational field.[22] The large discrepancies between length scales and amplitude scales between the aerodynamic motions and the acoustic fluctuations hence require the use of high-order schemes for both space and time discretizations. Following these guidelines, spatial derivatives are approximated using explicit 6th-order 7-point finite-differences. A selective filtering procedure is furthermore implemented in order to remove unwanted spurious perturbations. Spectral-like discrete filtering, based on a 6th-order 7-point stencil, is therefore applied to the flow variables.[3] To keep accuracy at its highest level, Lagrangian interpolation is performed thanks to 4th-order polynomials.[10] Finally, time integration of the solution is carried out by a 4th-order 6-step low-storage Runge-Kutta scheme, whose coefficients have been optimized in the Fourier space.[1] Subgrid-scale modeling is performed using explicit filtering of the flow variables. The dissipation provided by the unresolved scales is thus taken into account by removing energy at the smaller scales, close to the grid cut-off.[4,6]

II.C. Grid design

The computational domain is discretized by eight different structured meshes. The resulting composite grid allows to accurately capture the turbulent flow development as well as the radiated sound field.

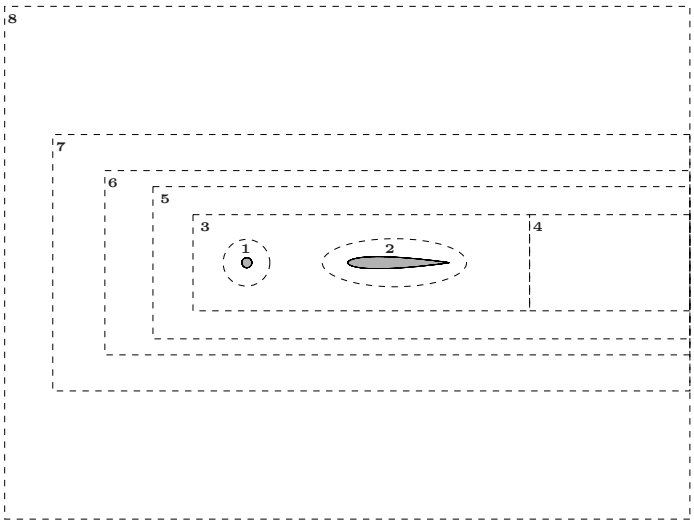

Figure 2. Sketch of the composite grid for the present rod-airfoil flow configuration (figure not to scale, overlapping regions not represented). 1: rod mesh, 2: airfoil mesh, 3: aerodynamic mesh, 4: sponge zone, 5, 6, 7: intermediate meshes, 8: acoustic mesh.

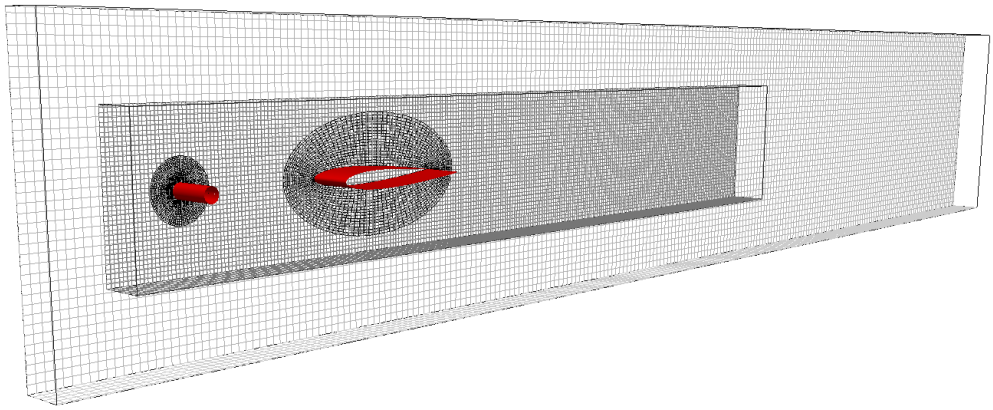

Figure 3. Overview of the meshes number 1, 2, 3 and 5 (see figure 2 for grid numbering).

A sketch of the rod-airfoil multi-grid is presented in figure 2 and a three-dimensional visualization of the meshes build for the aerodynamic region are proposed in figure 3. Following the works of Boudet *et al.*[7] or Greschner *et al.*[14] the domain is taken to be periodic in the spanwise direction and extends over 0.3 chord-length. Around the rod and the airfoil, body-fitted curvilinear meshes have been constructed (grid #1 and #2). Small mesh sizes have been chosen to ensure that all the features of wall turbulence are well reproduced. The first cell size normal to the wall is, in wall units, $\Delta y^+ \sim 2.5$ for the node on top of the rod at $x/c_h = -1$. Above the middle of the airfoil, at $x/c_h = 0.5$, the mesh is such as $\Delta y^+ \sim 3$. The rod and the airfoil are surrounded by an aerodynamic Cartesian mesh in order to connect them (grid #3). Downstream the aerodynamic mesh lies a sponge zone used to attenuate turbulent motions before they hit the outflow boundary condition (grid #4). An acoustic mesh (grid #8) is also present to propagate sound waves to the far field. The mesh size is given by $\Delta x = \Delta y = \Delta z = 8.5 \times 10^{-2} c_h$ so that the cut-off wavelength of the grid corresponds to a cut-off Strouhal number equal to $fd/U_\infty \sim 1.4$, *i.e.* $f = 10000$ Hz. In-between the aerodynamic and the acoustic meshes (grid #3 and #8, respectively) intermediate meshes (grid #5, #6 and #7) have been placed to perform a smooth transition between the mesh sizes of the aerodynamic and acoustic domains. To avoid stiff mesh size jumps, only mesh coarsening by an approximate factor of two is used. It should be also noted that the spanwise mesh size is also varied in order to reach mesh cells with an aspect ratio close to 1 in every direction.

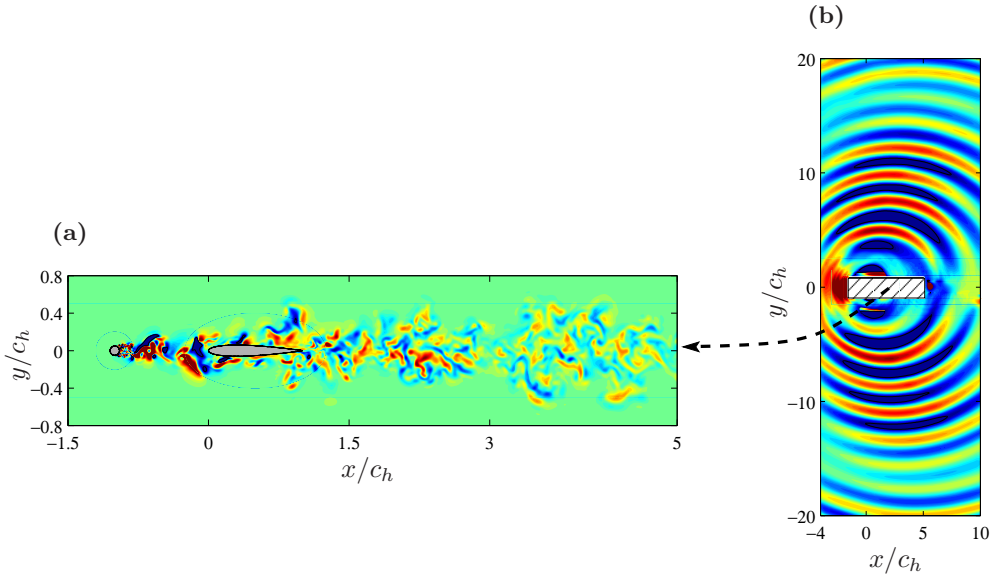

Figure 4. (a) Snapshot of the unsteady spanwise velocity field in the central plane of the computational domain. Colorscale from $-0.2U_\infty$ (blue) to $+0.2U_\infty$ (red). Gray surfaces represent solid bodies. (b) Snapshot of the fluctuating pressure field in the central plane of the computational domain. Colorscale from -50 Pa (blue) to $+50$ Pa (red). The dashed area corresponds to the flow region presented on the left.

The characteristics of the composite grid are compiled in table 1. The total number of mesh points is approximately 20×10^6. One may observe that there are two orders of magnitudes between the typical mesh sizes in the aerodynamic region and the one in the far-field acoustic domain. Such a mesh jump is achieved in a smooth manner thanks to the grid overlapping technique. It is worth noting that most of the grid nodes are clustered inside the aerodynamic region. The discretization of the far-field (grid #8) indeed only requires 1.5% of the total number of mesh points.

The whole domain extends over $[-4c_h\ ;\ 10c_h] \times [-20c_h\ ;\ 20c_h] \times [-0.15c_h\ ;\ 0.15c_h]$. The time step $\Delta t \sim 6.5 \times 10^{-8}$ s corresponds to a Courant-Friedricks-Levy number equal to 0.8. To ensure statistical convergence and to compute at least 100 periods of the vortex-shedding phenomena, the simulation is run over 10^6 iterations on 1024 processors.

III. Results and validation

III.A. Overview of the flow field

The flow development as predicted by the numerical simulation is first investigated in a qualitative manner. Snapshots of the unsteady flow field are presented and discussed in order to determine whether the gross features of the flow physics are indeed well reproduced.

The turbulent flow development is illustrated in figure 4.a where the instantaneous snapshot of the magnitude of the velocity field, taken in the central plane of the computational domain, is plotted. It is seen that turbulence ignition is indeed achieved by the rod and that the development in the near-wall region of unsteady motions eventually leads to the periodic shedding of large scale organized vortices in the wake of the cylinder. Due to the flow three-dimensionalization, smaller turbulent scales are also visible.

An overview of the radiated acoustic field is proposed in figure 4.b, where a snapshot of the pressure fluctuations in the central plane is plotted. A tonal noise component, associated with the periodic impingement of the rod wake on the airfoil, is clearly visible on either side of the rod-airfoil setup.

III.B. Mean flow field

Some mean flow quantities, namely mean velocities and turbulence intensities, are now faced with hot-wire data to check the consistency of the present results. Jacob *et al.*[17] pointed out that during their experiments the rod and the airfoil were not perfectly aligned. The rod is indeed a few millimeters (a few percent of the

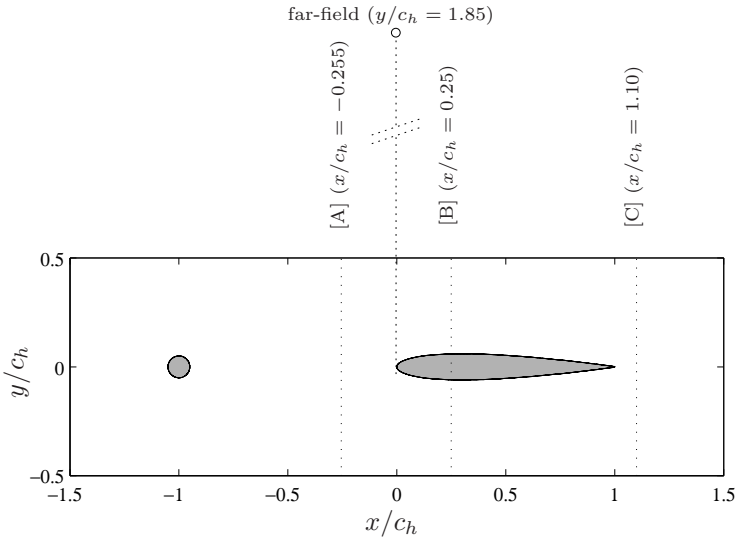

Figure 5. Sketch of the rod-airfoil configuration and of the measurement locations.

chord length) off in the transverse direction. Due to this bias into the experimental flow setup, discrepancies can be expected. One may nonetheless consider that the measurements of Jacob *et al.*[17] provide reliable references of the overall magnitude of the mean flow quantities.

The mean streamwise velocity $\overline{u}/U_\infty$ is represented in figure 6 as a function of the transverse coordinate y/c_h. Three streamwise locations, as shown in figure 5, referred to as section [A] ($x/c_h = -0.255$), section [B] ($x/c_h = 0.25$) and section [C] ($x/c_h = 1.1$) are plotted in figures 6.a, 6.b and 6.c, respectively. The experimental data of Jacob *et al.*[17] are presented for comparison. In-between the rod and the airfoil, in figure 6.a, a good collapse between the present results and the experimental data is observed. The wake width as well as the velocity defect at the center of the wake are well reproduced. Further downstream, above the profile, it is seen in figure 6.b that there is a fair agreement between the numerical data and the hot-wire profile. At this location the calculation turns out to overestimate the streamwise mean flow but the overall amplitude is nonetheless well predicted. Finally, the mean streamwise velocity in the wake of the airfoil, presented in figure 6.c, is also consistent with the hot-wire measurements. The gap between the experiments and the simulation is rather large for $y/c_h > 0$ but a very good collapse is visible for negative transverse locations. Recall that the experimental setup is not symmetric so that the hot-wire measurements are consequently not symmetric too.

The turbulent intensity $\sqrt{\overline{u'u'}}/U_\infty$ based on the mean streamwise velocity fluctuations is depicted in figure 6 as a function of the transverse coordinate y/c_h, for three streamwise locations : section [A] in figure 6.d, section [B] in figure 6.e and section [C] in figure 6.f. The experimental data of Jacob *et al.*[17] are also provided to assess the present LES results. Downstream the cylinder, in figure 6.d, the turbulent activity in the center of the wake is slightly overestimated by the present calculation but the overall agreement is good and few discrepancies can be seen between the two sets of data. In figure 6.e, the turbulent intensity above the airfoil provided by the simulation is slightly larger than that of the experiments. The error remains however within a few percents. Further downstream, in figure 6.f, turbulence activity in the wake of the airfoil is correctly predicted. In particular, as it was already reported for the mean streamwise velocity in figure 6.c, a better collapse with the reference data is observed for negative transverse locations.

III.C. Radiated acoustic field

The time evolution of the pressure fluctuations p' obtained at the location $(x/c_h, y/c_h) = (0, 18.5)$ in the far-field, as shown in figure 5, is presented in figure 7.a as a function of the normalized time tU_∞/d. It is seen that the signal is dominated by periodic oscillations with amplitudes slightly modulated in time. This tone noise is associated to the sound radiated by the periodic impingement of vortical structures on the airfoil leading edge.

The power spectral density (PSD) of the far-field pressure fluctuations is provided in figure 7.b as a

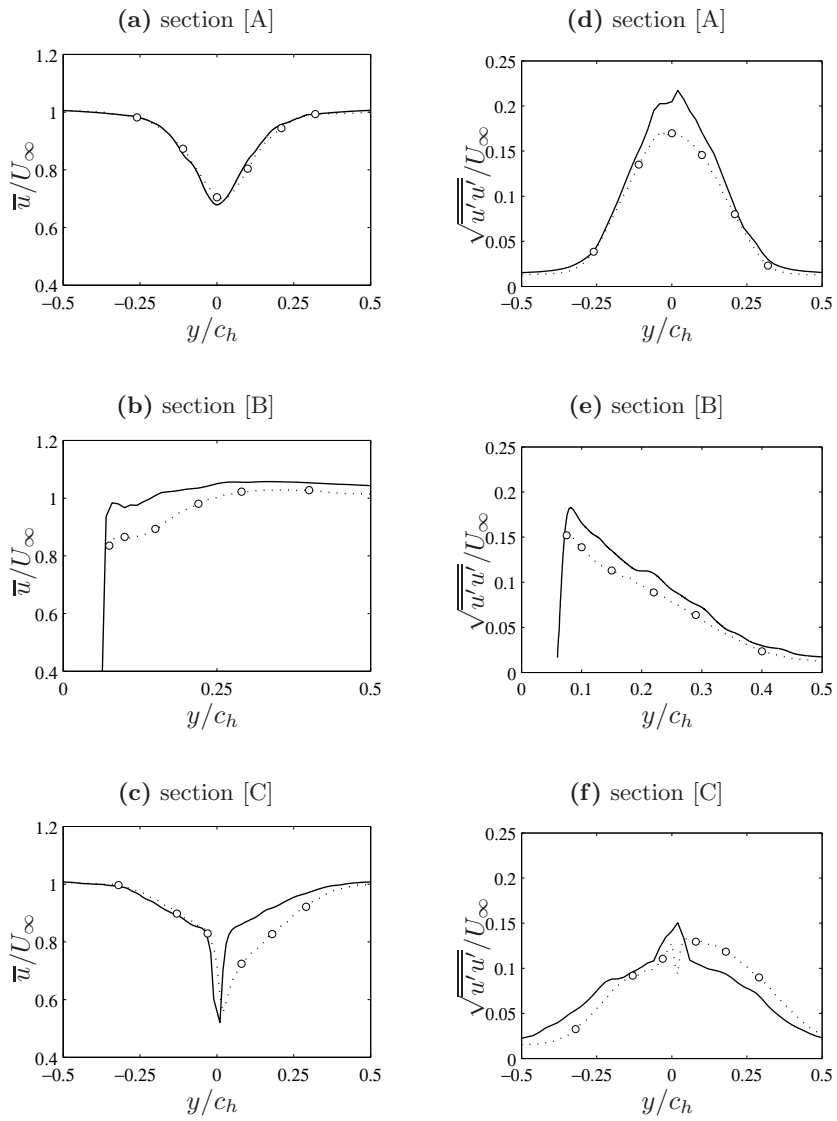

Figure 6. (a–c) Mean streamwise velocity $\overline{u}/U_\infty$ as a function of the transverse position y/c_h, and (d–f), mean streamwise turbulent intensity $\sqrt{\overline{u'u'}}/U_\infty$ as a function of the transverse position y/c_h, for various streamwise locations (see figure 5). ———, present LES; · · · ○ · · ·, experimental data.[17]

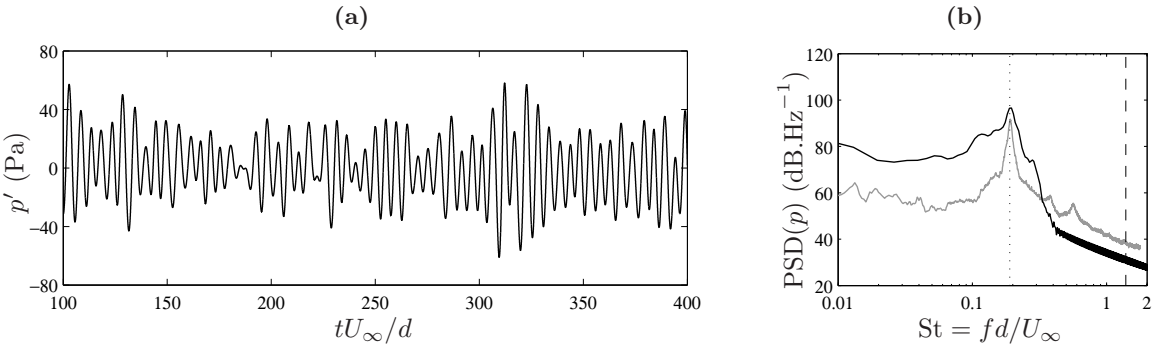

Figure 7. (a) Pressure fluctuation history in the far-field for an observer normal to the flow at a distance $R = 18.5c_h$ from the airfoil leading edge. (b) Power spectral density of the pressure perturbations measured in the far-field for an observer normal to the flow at a distance $R = 18.5c_h$ from the airfoil leading edge. The present LES results (black plot) are compared to the data provided by the experiments of Jacob *et al.*[17] (gray plot). The dotted line indicates the expected Strouhal number St $= 0.19$ of the vortex-shedding frequency behind the cylinder. The dashed line represents the mesh cut-off Strouhal number St $= 1.39$ in the far-field grid.

function of the Strouhal number St $= fd/U_\infty$ based on the cylinder diameter. The experimental data of Jacob *et al.*[17] are also plotted for comparison. A good collapse between numerical and experimental results is observed even though the half-width of the pic is overestimated. This trend is likely to be due to the discrepancies between the length of the signals of the simulation and of the experiments. Numerical calculation indeed provide relatively short time-resolved data. Nonetheless, as expected, the calculated spectrum exhibit a strong tonal component at the vortex shedding frequency and the predicted Strouhal number shows a very good agreement with the reference data. In addition the pressure level radiated by the harmonic pic is well reproduced. The gap between the simulation and the experiments remains small, about 4 dB.

IV. Conclusion

In the present paper, direct noise calculation of the sound sources of a rod-airfoil flow configuration has been performed. Using the specific solver *Code_Safari*,[12] the large-eddy simulation of the compressible Navier-Stokes equations using spectral-like numerical methods on a set of overlapping grids permitted to determine the turbulent flow development as well as the radiated sound field in a single calculation. Detailed comparisons to the experimental data of Jacob *et al.*[17] have been carried out to assess the consistency of the present computation. A good agreement between the reference data and the predicted results has been shown for the turbulence statistics and for the quasi-tonal sound radiation observed in the far-field. This study therefore demonstrates that the use of high-order discretization tools on overlapping structured grids permits to perform the direct noise calculation of the sound sources associated to the turbulent flow development around multiple bodies is feasible and yields accurate results.

As pointed out, among the numerous branches of the aeroacoustic computation field, direct calculation of the radiated acoustic is particularly reliable since it does not require any sound source modeling. It produces comprehensive data which can help understanding the flow physics of sound generation processes in turbulent flows. Future works on the rod-airfoil case include the study of the influence of the distance between the cylinder and the profile. Using the procedure described in this paper the direct impact on both acoustic and aerodynamic fields can be obtained and thoroughly investigated.

Acknowledgments

This work is supported by the "Agence National de la Recherche" under the reference ANR-06-CIS6-011 (project "STURM4").The authors wish to thank Dr. Bill Henshaw for his valuable recommendations concerning the overset strategy.

References

[1]Berland, J., Bogey, C., Bailly, C., Low-dissipation and low-dispersion fourth-order Runge-Kutta algorithm, *Comput. Fluids*, **35**, 1459-1463 (2006)

[2]Berland, J., Bogey, C., Bailly, C., Numerical study of screech generation in a planar supersonic jet, *Phys. Fluids*, **19**, #075105 (2007)

[3]Bogey, C., Bailly, C., A family of low dispersive and low dissipative explicit schemes for flow and noise computations, *J. Comput. Phys.*, **194**, 194-214 (2004)

[4]Bogey C., Bailly C., Large eddy simulations of round free jets using explicit filtering with/without dynamic Smagorinsky model, *Int. J. Mass Transfer*, **27**, 603 (2006).

[5]Bogey C., Bailly C., An analysis of the correlations between the turbulent flow and the sound pressure fields of subsonic jets, *J. Fluid Mech.*, **583**, 71 (2007).

[6]Bogey C., Bailly C., Turbulence and energy budget in a self-preserving round jet, *J. Fluid Mech.*, **627**, 129 (2009).

[7]Boudet J., Grosjean N., Jacob M.C., Wake-airfoil interaction as broadband noise source: a large-eddy simulation study, *Int. J. Aeroacoustics*, **4**(1), 93 (2005)

[8]Casalino, D., Jacob M.C., Roger M., Prediction of rod-airfoil interaction noise using the Ffowcs-Williams Hawkings analogy, *AIAA J.*, **41**(2), 182-191 (2003)

[9]Chessirre, G., Henshaw, W.D., Composite overlapping meshes for the solution of partial differential equations, *J. Comput. Phys.*, **90**, 1-64 (1990)

[10]Daude F., Emmert T., Lafon P., Crouzet F., Bailly C., A high-order algorithm for compressible LES in CAA applications, *Proceedings of the 14th AIAA/CEAS Aeroacoustics Conference*, 5-7 may, Vancouver, Canada, USA, AIAA Paper 2008-2873 (2008)

[11]Delfs, J.W., An overlapped grid technique for high resolution CAA schemes for complex geometries, *Proceedings of the 7th AIAA/CEAS Aeroacoustics Conference and Exhibit*, Maastricht, Netherlands, May 28-30, AIAA-Paper 2001-2199 (2001)

[12]Emmert, T., Lafon, P. & Baily, C., Numerical study of self-induced transonic flow oscillations behind a sudden duct enlargement, *Phys. Fluids*, **21**, 106105 (2009)

[13]Ffowcs Williams, J.E., Hawkings, D.L., Sound generated by turbulence and surfaces in arbitrary motion, *Phil. Trans. Roy. Soc.*, **A264**(1151), 321-342 (1969)

[14]Greschner B., Thiele F., Jacob M.C., Casalino D., Prediction of sound generated by a rod-airfoil configuration using EASM DES and the generalised Lighthill/FW-H analogy, *Comput. Fluids*, **27**, 402-413 (2008)

[15]Homicz G.F., George A.R., Broadband and discrete frequency radiation from subsonic rotors, *J. Sound Vib.*, **36**(2), 151 (1974)

[16]Kato C., Iida A., Takano Y., Fujita H., Ikegawa M., Numercial prediction of aerodynamic noise radiated from low Mach turbulent wake, *Proceedings of the 31st AIAA Aerospace Sciences Meeting and Exhibit*, 11-14 january, Reno, NV, USA, AIAA Paper 93-0145 (1993)

[17]Jacob M.C., Boudet J., Casalino J., Michard M., A rod-airfoil experiment as benchmark for broadband noise modeling, *J. Theoret. Comput. Fluid Dyn.*, **19**(3), 171 (2005).

[18]Lighthill, M., On sound generated aerodynamically, I, general theory, *Proc. Roy. Soc. London*, **A-211**, 564-587 (1952)

[19]Prewitt, N.C., Belk, D.M., Shyy, W., Parallel computing of overset grids for aerodynamic problems with moving objects, *Prog. Aerosp. Sci.*, **36**, 117-172 (2000)

[20]Sherer, S.E., Scott, J.N., High-order compact finite-difference methods on general overset grids, *J. Comput. Phys.*, **210**(2), 459-496 (2005)

[21]Takagi, Y., Fujisawa, N., Nakano, T., Nashimoto, A., Cylinder wake influence on the tonal noise and aerodynamic characteristics of a NACA0018 airfoil, *J. Sound Vib.*, **297**, 563-577 (2006)

[22]Tam, C.K.W., Computational aeroacoustics: issues and methods, *AIAA J.*, **33**, 1788-1797 (1995)

[23]Tam C.K.W., Dong Z., Radiation and outflow boundary conditions for direct computation of acoustic and flow disturbances in a nonuniform mean flow, *J. Comput. Acoust.*, **4**, 175 (1996)

[24]Wang, M., Freund, J.B., Lele, S.K., Computational prediction of flow-generated sound, *Ann. Rev. Fluid Mech.*, **38**, 483-512 (2006)

[25]Williamson C.H.K., Vortex dynamics in the cylinder wake, *Ann. Rev. Fluid Mech.*, **28**, 477 (1996).